

## Flow Cytometry as a New Approach To Investigate Drug Transfer between Lipid Particles

Silvia Petersen,<sup>†</sup> Alfred Fahr,<sup>†</sup> and Heike Bunjes<sup>\*‡</sup>

Department of Pharmaceutical Technology, Institute of Pharmacy,  
Friedrich-Schiller-Universität Jena, Jena, Germany, and Institute of Pharmaceutical  
Technology, Technische Universität Braunschweig, Braunschweig, Germany

Received May 11, 2009; Revised Manuscript Received December 7, 2009; Accepted January 11, 2010

**Abstract:** Lipid nanoparticles and liposomal carrier systems are of growing interest for intravenous drug delivery due to their biocompatibility and targetability. It is, however, difficult to investigate their release behavior for lipophilic drugs under physiological conditions. This study describes a novel flow cytometric method studying drug transfer from such carrier systems to particles simulating physiological receptor sites. For this purpose, liquid and solid trimyristin nanoparticles or soybean phospholipid liposomes were loaded with the lipophilic fluorescent substances Nile red, temoporfin, and Dil. The transfer of these model drugs to large emulsion droplets was examined by flow cytometry. Transfer of Dil to differently sized acceptor emulsions was also monitored by separating donor and acceptor particles using ultracentrifugation. Flow cytometry revealed a completion of transfer within a few minutes for Nile red and temoporfin at considerable amounts of transferred dye. In contrast, the highly lipophilic Dil transferred over a period of weeks only for a small percentage of the dye. Ultracentrifugation results confirmed this for Dil and indicated a dependence of transfer characteristics on the acceptor surface area. Nile red transfer into a bulk oil phase as alternative acceptor system was also very slow. Flow cytometry seems to be well suited to study the intrinsic transfer of fluorescent lipophilic substances, as no kinetic hindrances like dialysis bags nor separation steps are required. Additional detailed experiments will, however, be necessary to elucidate the prevalent transfer mechanisms completely.

**Keywords:** Drug release; drug transfer; lipid nanoparticles; liposomes; flow cytometry; ultracentrifugation

### Introduction

Colloidal carrier systems as lipid nanoparticles or liposomes are being intensively investigated regarding their suitability for delivering lipophilic compounds. Knowledge on the drug release behavior of such formulations is of great importance, e.g. concerning their targeting suitability after intravenous administration. Due to the required small size of the particles for this way of delivery, the estimation of

the *in vivo* drug release by *in vitro* methods is, however, not a straightforward task.

Methods which have been described to investigate the *in vitro* drug release of colloidal drug delivery systems include sample-and-separate methods, membrane-barrier methods, continuous-flow methods and several *in situ* methods.<sup>1</sup> The sample-and-separate methods involve filtration or centrifugation steps to separate the particles from the release media at different time points followed by drug determination in the

\* To whom correspondence should be addressed. Mailing address: Institute of Pharmaceutical Technology, TU Braunschweig, Mendelssohnstr. 1, 38106 Braunschweig, Germany. Tel: 0049-531-391-5657. Fax: 0049-531-391-8108. E-mail: Heike.Bunjes@tu-braunschweig.de.

<sup>†</sup> Friedrich-Schiller-Universität Jena.

<sup>‡</sup> Technische Universität Braunschweig.

(1) Washington, C. Drug release from microparticulate systems. In *Drugs and the Pharmaceutical Sciences 73 (Microencapsulation—Methods and Industrial Applications)*; Benita, S., Ed.; Marcel Dekker: New York, 1996; pp 155–181.

release medium.<sup>2–6</sup> Commonly reported problems are clogging of filters by small particles, drug binding to the filter material or instabilities of the investigated formulations due to the intense introduction of energy during the separation process.<sup>7,8</sup> A separation step is not required when membrane-barrier methods like dialysis in different variations are used.<sup>3,7,9</sup> However, a dialysis membrane separates the release medium and the particle containing formulation allowing only the drug to pass over into the release medium which is followed by analysis. Depending on the dialysis method, the limited size of the membrane surface area and violation of sink conditions can be critical factors often leading to highly distorted release results.<sup>3,10–12</sup> Continuous-flow methods utilize flow-through cells containing the particle formulation under investigation which is circulated with a release medium. Also this method is prone to filter clogging with all the negative consequences like varying flow conditions.<sup>7,10,13</sup> *In situ* methods offer the possibility to directly analyze the drug within the particle containing release medium thereby distinguishing between the released and nonreleased drug. In other words, these methods are sensitive only for either the released or the nonreleased drug. For example, the drug can be analyzed spectroscopically (e.g., UV/vis, fluorescence,

phosphorescence) or via polarography, which constricts the number of potential drug candidates.<sup>1,10,14</sup>

One common disadvantage of these *in vitro* drug release techniques is the use of aqueous release media, e.g. buffer solutions. In order to get closer to *in vivo* conditions, the buffered media can be supplemented with albumin, for example.<sup>2,15</sup> Nevertheless, these conditions are not representative for the situation in the bloodstream in which also a variety of lipophilic compounds (particularly in cell membranes and lipoproteins) can take up released drug substances. Furthermore, the low aqueous solubility of many of the drugs of interest complicates their analysis in aqueous media.

In an attempt to come closer to *in vivo*-like release conditions with special regard to intravenous administration, this study focuses on the release kinetics of fluorescent lipophilic model substances from nanoparticulate lipid carriers. Unlike as in common techniques, not the actual release of the substances from the carrier into an aqueous system is investigated, but a transfer from the carrier particles into lipophilic acceptor compartments in the form of oil-in-water (o/w) emulsion droplets. These acceptor droplets are intended to mimic lipophilic compounds present in the blood and thereby present a compartment in which the released lipophilic substance is soluble. In order to make the detection of the drug in acceptor particles possible by flow cytometry, an o/w emulsion containing large, cell sized droplets which are recognizable by a flow cytometer is used.<sup>16–18</sup> As only the acceptor droplets are detected (no significant interference of the small particles), separation steps with all the negative consequences described are not required and the transfer mixture can be analyzed *in situ* after dilution. The fluorescent model drugs in this study are Nile red, DiIC<sub>18</sub>(3) (DiI) and temoporfin. Usually, Nile red is used to localize lipid droplets within cells whereas the highly lipophilic dye DiI is employed to analyze membrane structures and dynamics.<sup>19–22</sup>

- (2) Magenheimer, B.; Levy, M. Y.; Benita, S. A new *in vitro* technique for the evaluation of drug release profile from colloidal carriers—ultrafiltration technique at low pressure. *Int. J. Pharm.* **1993**, *94*, 115–123.
- (3) Boyd, B. J. Characterization of drug release from cubosomes using the pressure ultrafiltration method. *Int. J. Pharm.* **2003**, *260*, 239–247.
- (4) Hu, F. Q.; Yuan, H.; Zhang, H. H.; Fang, M. Preparation of solid lipid nanoparticles with clobetasol propionate by a novel solvent diffusion method in aqueous system and physicochemical characterization. *Int. J. Pharm.* **2002**, *239*, 121–128.
- (5) Cui, F.; Shi, K.; Zhang, L.; Tao, A.; Kawashima, Y. Biodegradable nanoparticles loaded with insulin-phospholipid complex for oral delivery: Preparation, *in vitro* characterization and *in vivo* evaluation. *J. Controlled Release* **2006**, *114*, 242–250.
- (6) Zur Mühlen, A.; Schwarz, C.; Mehnert, W. Solid lipid nanoparticles (SLN) for controlled drug delivery—Drug release and release mechanism. *Eur. J. Pharm. Biopharm.* **1998**, *45*, 149–155.
- (7) D’Souza, S. S.; DeLuca, P. P. Methods to assess *in vitro* drug release from injectable polymeric particulate systems. *Pharm. Res.* **2006**, *23*, 460–474.
- (8) Chidambaram, N.; Burgess, D. J. A novel *in vitro* release method for submicron-sized dispersed systems. *AAPS PharmSci* **1999**, *1*, E11.
- (9) Henriksen, I.; Sande, S. A.; Smistad, G.; Agren, T.; Karlsen, J. *In vitro* evaluation of drug release kinetics from liposomes by fractional dialysis. *Int. J. Pharm.* **1995**, *119*, 231–238.
- (10) Washington, C. Drug release from microdisperse systems: a critical review. *Int. J. Pharm.* **1990**, *58*, 1–12.
- (11) D’Souza, S. S.; DeLuca, P. P. Development of a dialysis *in vitro* release method for biodegradable microspheres. *AAPS PharmSciTech* **2005**, *6*, E323–E328.
- (12) Levy, M. Y.; Benita, S. Drug release from submicronized o/w emulsion: a new *in vitro* kinetic evaluation model. *Int. J. Pharm.* **1990**, *66*, 29–37.
- (13) Washington, C.; Koosha, F. Drug release from microparticulates; deconvolution of measurement errors. *Int. J. Pharm.* **1990**, *59*, 79–82.
- (14) Rosenblatt, K. M.; Douromis, D.; Bunjes, H. Drug release from differently structured monoolein/poloxamer nanodispersions studied with differential pulse polarography and ultrafiltration at low pressure. *J. Pharm. Sci.* **2007**, *96*, 1564–1575.
- (15) Lanza, G. M.; Yu, X.; Winter, P. M.; Abendschein, D. R.; Karukstis, K. K.; Scott, M. J.; Chinen, L. K.; Fuhrhop, R. W.; Scherrer, D. E.; Wickline, S. A. Targeted antiproliferative drug delivery to vascular smooth muscle cells with a magnetic resonance imaging nanoparticle contrast agent. *Circulation* **2002**, *106*, 2842–2847.
- (16) Hai, M.; Bernath, K.; Tawfik, D.; Magdassi, S. Flow cytometry: a new method to investigate the properties of water-in-oil-in-water emulsions. *Langmuir* **2004**, *20*, 2081–2085.
- (17) Johnston, A. P. R.; Zelikin, A. N.; Lee, L.; Caruso, F. Approaches to quantifying and visualizing polyelectrolyte multilayer film formation on particles. *Anal. Chem.* **2006**, *78*, 5913–5919.
- (18) Sato, K.; Obinata, K.; Sugawara, T.; Urabe, I.; Yomo, T. Quantification of structural properties of cell-sized individual liposomes by flow cytometry. *J. Biosci. Bioeng.* **2006**, *102*, 171–178.
- (19) Gocze, P. M.; Freeman, D. A. Factors underlying the variability of lipid droplet fluorescence in MA-10 Leydig tumor cells. *Cytometry* **1994**, *17*, 151–158.

Temoporfin (Foscan) is an approved drug for the photodynamic therapy of head and neck cancer.<sup>23</sup>

As donor carrier systems, trimyristin nanoparticles and soybean phospholipid liposomes were chosen. Especially for the lipid nanoparticles, drug loading and release behavior may be expected to strongly depend on the physical state of the matrix lipid.<sup>24,25</sup> Prepared by melt-homogenization, trimyristin nanoparticles can exist in the form of supercooled liquid emulsion droplets when stored at room temperature (nanoemulsion). Storage at lower temperatures (e.g., in a refrigerator) results in crystallization of the matrix lipid and the formation of plateletlike structures (nanosuspension).<sup>24,26,27</sup> For some drugs the drug-loading capacity of supercooled nanoemulsions was shown to be higher than that of nanosuspensions but the incorporated drug has a high mobility in the liquid lipid resulting in a rapid release.<sup>2,24,28</sup> In contrast, the crystalline state of the lipid should immobilize the drug molecules, potentially leading to a sustained release profile.<sup>6,24</sup> During lipid crystallization the drug may, however, also be expelled into the aqueous phase or, alternatively, be enriched on the surface of the particles and thus be made easily available for release or transfer.<sup>6,24</sup>

In this study, we investigated the influence of the types of nanoparticle formulations on the release behavior as well as the effect of the lipophilicity of the loaded substances as this may also affect the release.<sup>29,30</sup> In addition to the flow

cytometric transfer investigations, a transfer study of Nile red from donor nanoparticles into a layer of medium chain triglycerides was conducted.<sup>25</sup> To obtain more detailed information on the transfer behavior of the systems containing the highly lipophilic dye DiI, additional transfer studies were carried out by ultracentrifuging mixtures of donor nanoparticles and acceptor emulsion droplets of different size.

## Experimental Section

**Materials.** The triglyceride trimyristin (Dynasan 114) was a gift of Condea Chemie, Witten, Germany, soybean phospholipid (Lipoid S75) was donated by Lipoid GmbH, Ludwigshafen, Germany, and medium chain triglycerides (Miglyol 812N) were a gift of Merck KGaA, Darmstadt, Germany. The surfactants poloxamer 188 (Lutrol F-68) and polyvinyl alcohol (Mowiol 3-83) were from BASF AG, Ludwigshafen, Germany, and Clariant GmbH, Frankfurt/Main, Germany, respectively. Glycerol and thiomersal were purchased from Caesar & Loretz, Hilden, Germany. Nile red (9-diethylamino-5*H*-benzo[*a*]phenoxazin-5-one) was obtained from Acros Organics, Geel, Belgium, and DiI (DiIC<sub>18</sub>(3), 1,1'-dioctadecyl-3,3',3'-tetramethylindocarbocyanine perchlorate) was from Invitrogen GmbH, Karlsruhe, Germany. Temoporfin (5,10,15,20-tetrakis(3-hydroxyphenyl)chlorin) was a kind gift from Biolitec AG, Jena, Germany. The solvents acetonitrile and tetrahydrofuran were from Fisher Scientific, Nidderau, Germany. All substances were used as received. Water was purified by reverse osmosis and subsequent distillation.

**Methods. Preparation of Donor Lipid Nanoparticles.** The dispersions contained 2% trimyristin and 1.6% poloxamer 188 in an aqueous phase isotonicized with 2.25% glycerol and preserved with 0.01% thiomersal (all concentrations w/w). The matrix lipid and the aqueous phase containing the surfactant were heated to 70 °C. After melting of the triglyceride, the aqueous phase was added and the mixture was prehomogenized (1 min, 24,000 rpm, Ultra-Turrax). This crude emulsion was transferred to the 70 °C warm high-pressure homogenizer (Microfluidizer M-110S, Microfluidics, Newton, MA) and treated for 3 min at 500 bar. The hot colloidal emulsion was allowed to cool to room temperature. Under these conditions the matrix lipid remains in its liquid state due to supercooling.<sup>26</sup>

Loading of these supercooled emulsion droplets with Nile red (1.6 µg/mL of the dispersion) was done by evaporation of an ethanolic stock solution (800 µg/mL) in a glass vial leaving behind a thin film of Nile red followed by addition of the nanoemulsion and shaking for at least 24 h. Loading with DiI (2.0 µg/mL of the dispersion) was conducted by direct addition of an ethanolic stock solution (200 µg/mL) to the nanoemulsion followed by shaking for 5 days. Temoporfin was loaded to the nanoemulsion (15.0 µg/mL or 1.5 mg/mL of the dispersion) as described for DiI but

- (20) Klinkner, A. M.; Bugelski, P. J.; Waites, C. R.; Loudon, C.; Hart, T. K.; Kerns, W. D. A novel technique for mapping the lipid composition of atherosclerotic fatty streaks by en face fluorescence microscopy. *J. Histochem. Cytochem.* **1997**, *45*, 743–753.
- (21) Axelrod, D. Carbocyanine dye orientation in red cell membrane studied by microscopic fluorescence polarization. *Biophys. J.* **1979**, *26*, 557–573.
- (22) Foley, M.; MacGregor, A. N.; Kusel, J. R.; Garland, P. B.; Downie, T.; Moore, I. The lateral diffusion of lipid probes in the surface membrane of *Schistosoma mansoni*. *J. Cell Biol.* **1986**, *103*, 807–818.
- (23) Lorenz, K. J.; Maier, H. Squamous cell carcinoma of the head and neck. Photodynamic therapy with Foscan. *HNO* **2008**, *56*, 402–409.
- (24) Westesen, K.; Bunjes, H.; Koch, M. H. J. Physicochemical characterization of lipid nanoparticles and evaluation of their drug loading capacity and sustained release potential. *J. Controlled Release* **1997**, *48*, 223–236.
- (25) Jennings, V.; Schäfer-Korting, M.; Gohla, S. Vitamin A-loaded solid lipid nanoparticles for topical use: drug release properties. *J. Controlled Release* **2000**, *66*, 115–126.
- (26) Bunjes, H.; Westesen, K.; Koch, M. H. J. Crystallization tendency and polymorphic transitions in triglyceride nanoparticles. *Int. J. Pharm.* **1996**, *129*, 159–173.
- (27) Westesen, K.; Drechsler, M.; Bunjes, H. Colloidal dispersions based on solid lipids. In *Food Colloids*; Dickinson, E., Miller, R., Eds.; Royal Society of Chemistry: Cambridge, 2001; pp 103–115.
- (28) Westesen, K. Novel lipid-based colloidal dispersions as potential drug administration systems—expectations and reality. *Colloid Polym. Sci.* **2000**, *278*, 608–618.
- (29) Takino, T.; Konishi, K.; Takakura, Y.; Hashida, M. Long circulating emulsion carrier systems for highly lipophilic drugs. *Biol. Pharm. Bull.* **1994**, *17*, 121–125.

- (30) Saarinen-Savolainen, P.; Järvinen, T.; Taipale, H.; Urtti, A. Method for evaluating drug release from liposomes in sink conditions. *Int. J. Pharm.* **1997**, *159*, 27–33.



using a methanolic stock solution (2 mg/mL or 15 mg/mL) and shaking for 24 h. Shaking was done at 23 °C in a shaking water bath. The fraction of dye bound to the nanoparticles was assumed to be 100%.

Either the loaded dispersions were stored at room temperature, thereby retaining the liquid state of the trimyristin droplets (= donor emulsion), or the droplets were crystallized into plateletlike particles by storage of the dispersion at refrigerator temperature ( $\sim 2-8$  °C; = donor suspension).<sup>26</sup> Sample names in the text are composed according to the intended use of the formulation (Do, donor; Ac, acceptor), physical state of the matrix lipid (Emu, emulsion (super-cooled liquid lipid); Susp, suspension (crystalline lipid)), batch number and loaded fluorescent dye (NR, Nile red; DiI, DiI<sub>C18</sub>(3); Temo, temoporfin). For example, DoEmu-1-NR is a donor lipid nanoemulsion of the first batch loaded with Nile red.

**Preparation of Donor Liposomes.** The liposomes were prepared from a stock solution of soybean phospholipid Lipoid S75 in chloroform (40 mg/mL) in a round-bottom flask. For loading with fluorescent dyes, small volumes of ethanolic Nile red stock solution (800 µg/mL) or of methanolic temoporfin stock solution (2 mg/mL or 15 mg/mL) were added to the phospholipid solution. The organic solvents were evaporated using a stream of nitrogen and the remaining lipid film was rehydrated with hepes buffer (10 mM, pH 7.4) to a final concentration of 2% (w/w) phospholipid. The dye concentrations in the liposomal dispersions were 1.6 µg/mL for Nile red and 15.0 µg/mL or 1.5 mg/mL for temoporfin, respectively. After complete rehydration the dispersions were extruded for 21 times through a 100 nm polycarbonate membrane filter using a Liposofast extruder (Avestin Europe GmbH, Mannheim, Germany).

Sample names in the text are composed as described for the donor lipid nanoparticles: e.g., DoLip-1-NR is the donor liposome formulation of the first batch loaded with Nile red. The fraction of dye bound to the liposomes was assumed to be 100%.

**Preparation of Acceptor O/W Emulsions.** The acceptor o/w emulsions were composed of 5% (w/w) liquid medium chain triglycerides stabilized with 3% (w/w) polyvinyl alcohol in an aqueous phase containing 2.25% glycerol and 0.01% thiomersal. Homogenization was done at room temperature using an Ultra-Turrax (T 25, Jahnke & Kunkel, Staufen, Germany) at 24,000 rpm for 15 min. In order to prevent droplet coalescence, the emulsions were stored under gentle agitation in a rotary drying oven with 6 rpm at ambient temperature.

For calibration of the flow cytometer, small fractions of the emulsions were loaded with different amounts of the investigated fluorescent dyes in the same way as described for the donor lipid nanoparticles and also stored under agitation. For the centrifugation studies, acceptor emulsions with the same composition but different particle sizes were prepared either by high-pressure homogenization (Micro-fluidizer M-110S for 3 min at 150 to 500 bar) or by

homogenization with an Ultra-Turrax with differently sized dispersing tools at 24,000 rpm for 15 min.

Sample names in the text are composed as described for the donor lipid nanoparticles. AcEmu-3-DiI for instance is an acceptor emulsion from the third batch loaded with DiI used for the calibration of the flow cytometer, whereas AcEmu-3 is the same acceptor emulsion without DiI used for the transfer investigations.

**Particle Size Analysis.** Particle sizes of the donor particles were measured by photon correlation spectroscopy (PCS) using a Zetasizer Nano ZS (Malvern Instruments Ltd., Worcestershire, U.K.). The dispersions were diluted with filtered demineralized water and measured at 25 °C at a scattering angle of 173°. The results are given as the *z*-average diameter (*z*-ave, intensity weighted mean diameter assuming spherical particles) and the polydispersity index (PI, measure for the relative width of the particle size distribution). Three consecutive measurements of 5 min duration were averaged.

The particle sizes of the acceptor o/w emulsions were measured with laser diffraction (LD) in combination with PIDS (polarization intensity differential scattering) using a Coulter LS 230 particle sizer (Beckman Coulter Inc., Fullerton, CA). Eight consecutive measurements of 90 s were averaged. The applied evaluation model used the Mie theory with a refractive index of 1.332 for water and 1.45 for the sample. The volume distributions of the samples were calculated, and the results are given as the mean and the median particle sizes. Additionally, the specific surface area was calculated assuming a sample density of 1 g/mL.

**Investigation of Dye Transfer Using Flow Cytometry.** The transfer experiments were conducted using an Epics XL MCL flow cytometer (Beckman Coulter Inc., Fullerton, CA). Fluorescence excitation was done at 488 nm. The emitted fluorescence of the different dyes was detected at the corresponding photomultiplier tubes (PMT) after passing several filters. PMT FL2 was used to detect DiI after passing a 575 nm bandpass filter, PMT FL3 was used to detect Nile red or high concentrations of temoporfin after passing a 620 nm bandpass filter, and PMT FL4 was used to detect temoporfin in low concentrations after passing a 675 nm bandpass filter.

The transfer of the fluorescent dyes was investigated by mixing dye loaded donor dispersion (nominally 20 mg/mL lipid) with unloaded acceptor emulsion (50 mg/mL lipid) at different lipid mass ratios (LMR), which means that 1 mL of the acceptor emulsion was mixed with 100 µL, 20 µL, or 10 µL of the donor formulation. Nominally, the LMRs were chosen to be 1 + 25, 1 + 125, and 1 + 250 (= LMR<sub>nom</sub>), respectively, but as the determination of lipid content of the donor nanoparticles (see Supporting Information) was done only after the transfer experiments, the real LMRs (= LMR<sub>real</sub>) deviated from the intended ones in most cases. For example, LMR<sub>real</sub> of 1 + 22 or 1 + 112 were applied instead of LMR<sub>nom</sub> of 1 + 25 or 1 + 125, respectively. Usually, the mixtures were subsequently stirred at 23 °C on a stirring plate (350 rpm), but the mixtures for investigating

the transfer of DiI were agitated at 23 °C or at 37 °C in a shaking water bath. The transfer of Nile red was also investigated in highly diluted systems: Under stirring, 90.9  $\mu\text{L}$  of unloaded acceptor emulsion was added to 29.9 mL or to 299.9 mL of purified water as external phase, respectively. Finally, 9.1  $\mu\text{L}$  of the donor formulation was added ( $\text{LMR}_{\text{nom}} 1 + 25$ ; dilution donor/acceptor-water 1 + 299 or 1 + 2999, respectively). Samples were collected at different time points after mixing. Five to 10  $\mu\text{L}$  of the mixture were diluted in purified water and directly measured. 10,000 droplets were counted at a count rate of about 250 droplets per second. Between the measurements cleaning steps were introduced in order to avoid mixing with residual droplets of preceding samples using a special cleaning solution (Coulter Clenz Cleaning Agent, Beckman Coulter GmbH, Krefeld, Germany) and purified water. The transfer behavior of Nile red and temoporfin was investigated for less than one hour whereas the transfer experiments for DiI were performed for several weeks. A calibration of the flow cytometer was done for each acceptor emulsion and each dye under investigation by diluting and subsequent measuring of acceptor samples which were loaded with defined amounts of dye. The amount of dye transferred into the acceptor during the experiments was calculated from the calibration function.

A macroscopic exponential function was used to describe the transfer curves of the percental transferred amount of dye by using the nonlinear fitting algorithm of Microcal Origin 6.0 software (OriginLab Corporation, Northampton, MA):

$$A_{\text{acc}} = A_{\text{final}} - A \times e^{-k \times t} \quad (1)$$

$A_{\text{acc}}$  is the percental amount of dye transferred to the acceptor emulsion at time  $t$ ,  $A_{\text{final}}$  is the final percental transferred amount of dye and marks the height of the plateau,  $A$  is a pre-exponential coefficient and  $k$  is the rate constant of the transfer and thus a measure of the transfer rate. In the following, low  $A_{\text{final}}$  values are referred to as a less pronounced transfer, which took place to a small extent or ended at a low plateau level. High  $A_{\text{final}}$  values are referred to as a transfer which was pronounced, took place to a large extent or ended at a high plateau level. Low  $k$  values are referred to as a slow transfer whereas high  $k$  values are referred to as a rapid or fast transfer. Statistical analysis was performed using Student's  $t$  test to compare  $A_{\text{final}}$  values and to compare the rate constants  $k$ .

*Investigation of Nile Red Transfer into a Layer of Liquid Oil (Well Plate Transfer Study).* Similar to the release studies described by Jennings et al.<sup>25</sup> 500  $\mu\text{L}$  of donor emulsion or suspension labeled with Nile red were pipetted into each well of 24-well plates. Subsequently, the nano-particle dispersion was carefully covered with a layer of 1 mL of medium chain triglycerides. The plates were wrapped in tinfoil and gently shaken with 125 rpm on a plate shaker at room temperature ( $\sim 23$  °C). For sample collection, plates were removed from the shaker and three 100  $\mu\text{L}$

samples of the medium chain triglyceride cover layer of one well were collected and pipetted each into a black 96-well plate. Sample collection started 30 min after covering the donor dispersions with medium chain triglycerides and was stopped after 191 h.

The Nile red fluorescence of the oil samples in the 96-well plates was measured with a plate reader (Fluostar optima, BMG Labtechnologies, Offenburg, Germany) with an excitation wavelength of 544 nm and an emission wavelength of 645 nm. Each well was measured three times, and an average of 9 wells was calculated. For calibration, known concentrations of Nile red in medium chain triglycerides were measured under the same conditions as for the samples.

*Ultracentrifugation of Donor–Acceptor Mixtures Containing DiI.* Ultracentrifugation studies were performed by mixing 100  $\mu\text{L}$  of a donor suspension (7  $\mu\text{g/mL}$  DiI) with acceptor emulsions of different particle size (1 mL,  $\text{LMR}_{\text{nom}} 1 + 25$ ). The dye was allowed to transfer from donor to acceptor during a shaking time of 6 h or 32 days in a shaking water bath at ambient temperature. Subsequently, samples were diluted with purified water ( $\sim 11$  mL) into ultracentrifugation tubes. Samples were centrifuged (XL-80 ultracentrifuge, rotor type 70.1 Ti, Beckman Coulter Inc., Fullerton, CA) for 30 min at 15,000 rpm and additionally for 1 h at 25,000 rpm. In order to obtain a reference value (100%) the donor suspension was diluted and centrifuged without addition of acceptor emulsion. Furthermore, a mixture of donor suspension plus the acceptor emulsion with the largest particle size was centrifuged directly after preparing the mixture. This “recovery test” was done to account for sample losses due to an adhesive effect of the PVA introduced to the mixture in the acceptor emulsion. Using this method, about 91% of DiI could be recovered from the dye introduced with the donor suspension.

The acceptor emulsion cream layer on top of the tube and the donor suspension pellet were visually characterized. After removing the cream layer and aqueous supernatant the donor pellet was scraped from the tube bottom, resuspended in 200  $\mu\text{L}$  of water and sonicated for 2 min. The suspension was transferred into a glass vial, and the centrifugation tube was rinsed with ethanol (3 times 500  $\mu\text{L}$ ) added into the glass vial. The ethanol–water mixture was evaporated under a stream of nitrogen, and the pellet was dissolved in 1 mL of a mixture of acetonitrile–tetrahydrofurane 20:80 (v/v). DiI absorbance was measured at a wavelength of 551 nm, and the absorbance values of 6 measurements of 3 samples were averaged.

## Results

**Characteristics of Donor and Acceptor particles.** DSC investigations confirmed the physical state of the donor lipid nanoparticles (emulsions or suspensions; see Supporting Information). The PCS  $z$ -average particle sizes of the donor lipid nanoparticle formulations (prepared as different batches) were between 130 and 165 nm with corresponding PIs

**Table 1.** PCS Particle Sizes (z-Average Diameter) and Polydispersity Indices (PI) of the Donor Formulations

formulation	z-average [nm]/PI <sup>a</sup>			
	unloaded	loaded with Nile red	loaded with Dil	loaded with temoporfin
DoEmu-1	137/0.15	137/0.15	138/0.16	
DoSusp-1	151/0.21	152/0.22	150/0.21	
DoEmu-2	133/0.15	133/0.16		
DoSusp-2	146/0.21	146/0.21		
DoEmu-3	137/0.15	138/0.15		138/0.14; <sup>b</sup> 135/0.16 <sup>c</sup>
DoSusp-3	151/0.20	151/0.21		151/0.21; <sup>b</sup> 148/0.21 <sup>c</sup>
DoEmu-4	146/0.15	146/0.15		
DoSusp-4	163/0.21	163/0.21		
DoEmu-5	140/0.15		138/0.15	
DoSusp-5	155/0.21		154/0.21	
DoLip-1		105/0.08		
DoLip-2 <sup>b</sup>				102/0.07
DoLip-3 <sup>c</sup>				110/0.07

<sup>a</sup> All standard deviations were below 0.7 nm (z-average) and below 0.007 (PI). <sup>b</sup> 15  $\mu\text{g/mL}$ . <sup>c</sup> 1.5 mg/mL (1.3 mg/mL for DoLip-3-Temo (see Supporting Information)).

between 0.15 and 0.22 (Table 1). As spherical particle shapes are assumed in the algorithm of the z-average diameter estimation, the crystalline platelets of the donor suspension yielded marginally larger particle sizes and PIs in comparison to the liquid droplets of the donor emulsion.<sup>26</sup> The data presented in Table 1 were obtained on the day of preparation of the donor emulsions or at the latest after one day of storage of the dispersions at refrigerator temperature to obtain crystalline donor suspension particles. During the time of use of the formulations for the transfer experiments there were no significant changes in the particle sizes (at most  $\pm 2$  nm) and PIs (at most  $\pm 0.01$ ). Drug loading had no significant effect on the particle size of the lipid nanoparticles. The donor liposomes had PCS z-average particle sizes between 100 and 110 nm with PIs between 0.07 and 0.08. Again, there was no shift in particle sizes or PIs during the time of use of the formulations.

Acceptor emulsions prepared for investigations with the flow cytometer (AcEmu-1 to AcEmu-4) showed median particle sizes between 7.8 and 11.2  $\mu\text{m}$  according to laser diffractometry (Table 2).

Acceptor emulsions prepared for ultracentrifugation studies (AcEmu-5 to AcEmu-9) showed decreasing median laser diffraction particle sizes from 8.6 to 0.1  $\mu\text{m}$  accompanied by a corresponding increase in the specific surface area. Also the acceptor emulsion droplets exhibited no remarkable changes of their characteristic particle size values within the time frame of the experimental use.

#### Investigation of Dye Transfer Using Flow Cytometry.

**Method Development.** Prior to the transfer investigations, several evaluation steps for this new method were performed. Details on the instrumental adjustment can be found in the Supporting Information. Stable o/w acceptor emulsion droplets were developed which were sufficiently large for detection by flow cytometry. Their median droplet size (7.8 to 11.2  $\mu\text{m}$ ) fitted well into the size detection range of the

**Table 2.** Characteristic Particle Sizes and Specific Surface Areas of the Acceptor Emulsions According to Laser Diffraction + PIDS

	particle size [ $\mu\text{m}$ ]		specific surface area [ $\text{m}^2/\text{mL}$ ] <sup>a</sup>
	mean	median	
AcEmu-1	8.50	9.73	0.04
AcEmu-2	9.39	11.2	0.04
AcEmu-3	7.29	7.82	0.05
AcEmu-4	8.41	9.75	0.05
AcEmu-5	7.74	8.64	0.05
AcEmu-6 <sup>b</sup>	1.24	1.54	0.47
AcEmu-7 <sup>c</sup>	0.21	0.26	1.86
AcEmu-8 <sup>c</sup>	0.16	0.17	2.21
AcEmu-9 <sup>c</sup>	0.11	0.11	3.02

<sup>a</sup> Specific surface area was calculated assuming a sample density of 1 g/mL containing 50 mg/mL lipid. <sup>b</sup> Prepared with a larger dispersing tool. <sup>c</sup> Prepared by high-pressure homogenization.

flow cytometer used in this study (0.5 and 40  $\mu\text{m}$ ).<sup>31</sup> Several tests confirmed that the small donor particles (PCS z-average diameter  $< 0.2$   $\mu\text{m}$ ) do not interfere with the measurement (see Supporting Information). The measurement results, which are displayed as fluorescence intensity by the flow cytometer, could be quantified after calibration (performed by measuring acceptor droplets loaded with different amounts of dye after dilution in water; see Supporting Information). A linear correlation between the amount of dye in the acceptor and the detected fluorescence intensity was obtained in all cases (Supplemental Figure II in the Supporting Information). This simple and fast way of calibration was specific for the respective acceptor emulsion and the respective dye.

**Transfer of Nile Red.** After mixing Nile red loaded donor formulations and acceptor emulsion ( $\text{LMR}_{\text{real}} 1 + 22$  for

(31) Beckman Coulter Inc. Epics XL and XL MCL Flow Cytometry Systems. <http://www.beckmancoulter.com/literature/Bioresearch/DS-10610.pdf> (accessed 08/06/02), part of Flow Cytometry. <http://www.beckmancoulter.com/> (accessed 08/06/02).

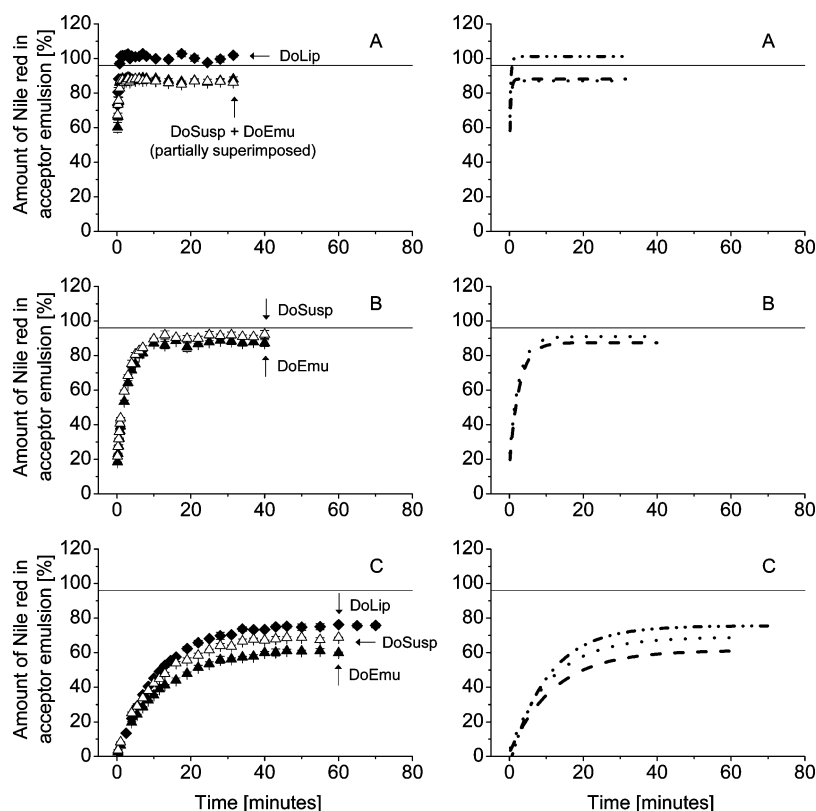


**Figure 1.** Transfer of Nile red from donor nanoparticles and donor liposomes to acceptor emulsion (LMR<sub>nom</sub> 1 + 25). 100% dye in AcEmu correspond to 0.16  $\mu$ g Nile red. Measurement results (left,  $n = 3$ ), fitted curves (right),  $\blacktriangle$  or dashed line = DoEmu,  $\triangle$  or dotted line = DoSusp,  $\blacklozenge$  or dashed-dotted line = DoLip, continuous line = equal distribution of Nile red between donor and acceptor. (A) “undiluted” experiments (LMR<sub>real</sub> 1 + 22 for DoEmu/DoSusp, 1 + 25 for DoLip), the results are representative for four different batches of DoEmu/DoSusp and AcEmu. (B) dilution to 30 mL (LMR<sub>real</sub> 1 + 28). (C) dilution to 300 mL (LMR<sub>real</sub> 1 + 28 for DoEmu/DoSusp, 1 + 25 for DoLip). Symbols are superimposed in some cases (rising part of the curves, DoEmu and DoSusp in A and B). For further details see Table 3.

DoEmu/DoSusp, 1 + 25 for DoLip) the amount of dye detected in the acceptor emulsion particles increased very rapidly, soon reaching a maximum value (Figure 1A). The transfer seemed to be completed after less than 2 min without significant differences in the height of the plateau ( $A_{\text{final}}$ ) between donor emulsion and suspension (Table 3, Supplemental Figure IV in the Supporting Information). The results presented in Figure 1A are representative for investigations carried out with, in total, four different batches of donor nanoparticles and acceptor emulsions (see Supplemental Figure III in the Supporting Information). The plateau of the donor liposomes was at a higher Nile red concentration. The rate constants ( $k$ ) were not significantly different for all three donor formulations. Assuming an equal distribution of the introduced 0.16  $\mu$ g of Nile red (= 100%) between the lipid matrices of donor and acceptor, about 96% of the Nile red would be expected within the acceptor emulsion (= calculated plateau value). The actual plateaus were 87 to 88% for the donor lipid nanoparticles and 101% for the donor liposomes. Thus, the Nile red affinity for the respective formulation seems to increase from donor liposomes to acceptor emulsion to donor lipid nanoparticles.

Additionally, the transfer of Nile red into acceptor droplets was investigated in diluted transfer mixtures (Table 3, Figure 1B,C, Supplemental Figure IV in the Supporting Information). Donor formulations were mixed with acceptor emulsion in varying amounts of water (LMR<sub>real</sub> 1 + 28 for DoEmu/DoSusp, 1 + 25 for DoLip). Dilution to 30 mL of water distinctly slowed down the transfer with the plateau only starting after approximately 10 min. Again, the donor lipid nanoparticles had the same transfer rate but, compared to the nondiluted experiments, the transfer from the donor suspension ended at a slightly lower plateau level than from the donor emulsion ( $A_{\text{final}}$ : 91% vs 87%). By increasing the water volume to 300 mL a further decrease of the transfer rate was observed. The plateau was only reached after more than 30 min and had an even lower level, presumably because a fraction of Nile red partitioned into the large aqueous volume. At this high dilution, the transfer from the donor suspension ended at a markedly higher plateau level than the transfer from the donor emulsion. A slower transfer was also observed for the donor liposomes but, as in the “undiluted” experiment, it occurred to a larger extent than



**Table 3.** Comparison of the Finally Released Percentual Amount of Nile Red ( $A_{\text{final}}$ ) and the Rate Constants ( $k$ ) for Nile Red Transfer into Acceptor Emulsions (Flow Cytometry) or into a Medium Chain Triglyceride Cover Layer (Well Plates) Assuming Transfer Kinetics According to Eq 1

type of experiment	formulations used	donor emulsion	donor suspension	donor liposomes
$A_{\text{final}} [\%]^a$				
“undiluted” <sup>b</sup>	DoEmu/DoSusp-1-NR and DoLip-1-NR to AcEmu-1	88.1 ± 1.8	87.1 ± 1.4	101.2 ± 1.9
diluted to 30 mL <sup>b</sup>	DoEmu/DoSusp-2-NR to AcEmu-2	87.4 ± 1.6	91.0 ± 1.6	
diluted to 300 mL <sup>b</sup>	DoEmu/DoSusp-2-NR to AcEmu-2 and DoLip-1-NR to AcEmu-1	61.3 ± 1.6	69.0 ± 1.9	75.6 ± 1.3
well plate transfer <sup>c</sup>	DoEmu/DoSusp-4-NR to oil cover layer	100.6 ± 12.1	106.4 ± 5.7	
$k [\text{min}^{-1}]^a$				
“undiluted” <sup>b</sup>	DoEmu/DoSusp-1-NR and DoLip-1-NR to AcEmu-1	2.9 ± 1.5	2.5 ± 1.4	2.9 ± 1.5
diluted to 30 mL <sup>b</sup>	DoEmu/DoSusp-2-NR to AcEmu-2	$3.8 \times 10^{-1} \pm 0.5 \times 10^{-1}$	$3.9 \times 10^{-1} \pm 0.5 \times 10^{-1}$	
diluted to 300 mL <sup>b</sup>	DoEmu/DoSusp-2-NR to AcEmu-2 and DoLip-1-NR to AcEmu-1	$8.3 \times 10^{-2} \pm 0.9 \times 10^{-2}$	$9.0 \times 10^{-2} \pm 1.1 \times 10^{-2}$	$9.7 \times 10^{-2} \pm 0.7 \times 10^{-2}$
well plate transfer <sup>c</sup>	DoEmu/DoSusp-4-NR to oil cover layer	$6.0 \times 10^{-4} \pm 2.6 \times 10^{-4}$	$8.3 \times 10^{-4} \pm 1.8 \times 10^{-4}$	

<sup>a</sup> Fitted mean and standard deviation. <sup>b</sup> Transfer into acceptor emulsions investigated by flow cytometry. <sup>c</sup> Transfer into a cover layer of medium chain triglycerides in well plates.

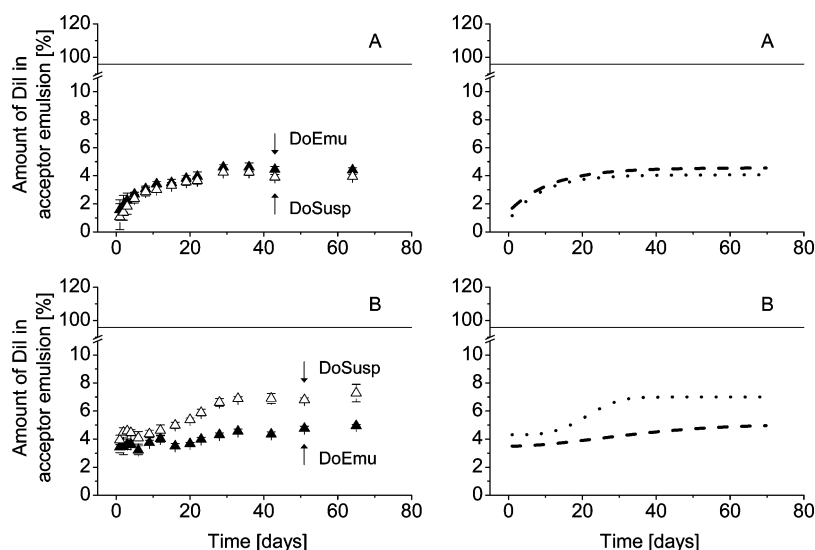


**Figure 2.** Transfer of DiI from donor nanoparticles to acceptor emulsion ( $\text{LMR}_{\text{nom}} 1 + 25$ ,  $\text{LMR}_{\text{real}} 1 + 22$ ). 100% dye in AcEmu correspond to  $0.2 \mu\text{g}$  DiI. Measurement results (left,  $n = 12$  (A) or  $n = 9$  (B)), fitted curves (right),  $\blacktriangle$  or dashed line = DoEmu,  $\triangle$  or dotted line = DoSusp, continuous line = equal distribution of DiI between donor and acceptor. (A) experiments performed at 23 °C. (B) experiments performed at 37 °C. In the rising part of the curves some results are superimposed. For further details see Table 4.

from the donor nanoparticles. In these highly diluted transfer mixtures the transfer rates increased from donor emulsion to suspension to liposomes.

**Transfer of DiI.** The transfer of DiI from donor lipid nanoparticles into acceptor emulsion droplets was investigated over more than two months at two different temperatures (23 and 37 °C,  $\text{LMR}_{\text{real}} 1 + 22$ ). For both donor formulations at 23 °C and for the donor suspension at 37 °C

the amount of transferred DiI steadily increased over the first 4 weeks of the experiment but it changed only slightly during the last weeks (Figure 2). In all cases, the amount of transferred DiI was below 7% ( $0.2 \mu\text{g} = 100\%$ ) and thus remained far away from the calculated equilibrium value ( $\sim 96\%$ ). The donor formulations incubated at 37 °C released a relatively high amount of DiI directly during the first day. During the following period of investigation, the released



**Table 4.** Comparison of the Finally Released Percentual Amount of Dil ( $A_{\text{final}}$ ) and the Rate Constants ( $k$ ) for Dil Transfer into Acceptor Emulsions at Two Different Temperatures

formulations used	$A_{\text{final}}$ [%] <sup>a</sup>	$k$ [days <sup>-1</sup> ] <sup>a</sup>
Experiments at 23 °C		
DoEmu-1-Dil to AcEmu-3	4.6 ± 0.4	$8.7 \times 10^{-2} \pm 4.3 \times 10^{-2}$
DoSusp-1-Dil to AcEmu-3	4.1 ± 0.4	$11.3 \times 10^{-2} \pm 5.4 \times 10^{-2}$
Experiments at 37 °C		
DoEmu-1-Dil to AcEmu-3 <sup>b</sup>	5.0 ± 2.2	$2.6 \times 10^{-2} \pm 4.2 \times 10^{-2}$
DoSusp-1-Dil to AcEmu-3 <sup>b</sup>	7.0 ± 0.4	$4.2 \times 10^{-2} \pm 0.8 \times 10^{-2}$

<sup>a</sup> Fitted mean and standard deviation. <sup>b</sup> Sigmoidal fit function applied (eq 2).

amount from the donor emulsion only changed marginally resulting in a smooth transfer course. This curve and the obviously sigmoidal transfer curve of the donor suspension could not be described by a simple exponential function as before. In order to parametrize also this set of curves a sigmoidal fit function was applied to the transfer curves at 37 °C:

$$A_{\text{acc}} = A_{\text{final}} - (A_{\text{final}} - A_0) \times e^{-(kt)^a} \quad (2)$$

The parameters are equal to eq 1 (Table 4, Supplemental Figure V in the Supporting Information).  $A_0$  is the amount of dye at time zero (= amount of dye transferred during the first day) and  $a$  is the power of the term  $kt$ .

Using eq 2 to fit the donor emulsion data obtained at 37 °C turned out to work better than using eq 1, but still the result was poor as is reflected in the high standard deviations. This causes the rate constants of donor emulsion and suspension to be statistically not significantly different. Nevertheless, the transfer from the donor suspension took place to a larger extent than from the donor emulsion. In contrast, the results obtained at 23 °C indicated a slightly higher transfer from the donor emulsion and again showed no differences in the transfer rates. No matter which temperature was applied, the plateaus of the donor emulsion did not differ whereas the plateau of the donor suspension at 37 °C was significantly higher than at 23 °C. The transfer rate for both formulations at 37 °C was lower compared to 23 °C.

**Transfer of Temoporfin.** Mixtures of donor formulations containing 15 µg/mL temoporfin and acceptor emulsion ( $\text{LMR}_{\text{real}}$  1 + 22 for DoEmu/DoSusp, 1 + 25 for DoLip) showed a rapid initial increase in the transferred amount of drug as seen before for Nile red (Figure 3A). The transfer rate of temoporfin (Table 5, Supplemental Figure VI in the Supporting Information) in this experiment was slightly lower than that of Nile red (“undiluted” experiments, Table 3). As for Nile red, the amount of transferred temoporfin increased from donor emulsion to suspension to liposomes. The calculated plateau value was again expected at about 96%

(assumption: equal distribution of 1.5 µg of temoporfin (=100%) between donor and acceptor). None of the plateau values was close to this state (DoEmu, ~25%; DoSusp, ~30%; DoLip, ~40%).

The temoporfin concentration in the donor formulations could be increased to 1.5 mg/mL (nanoparticles) or 1.3 mg/mL (liposomes, see Supporting Information), corresponding to concentrations used for therapy. Using the same  $\text{LMR}_{\text{real}}$  as for the low temoporfin concentration, the transfer curves again showed a very rapid initial increase (Figure 3B, Table 5, Supplemental Figure VI in the Supporting Information). The transfer was faster and more pronounced than from the formulations with the low temoporfin concentration but was again completed within the first minutes after mixing. Using this 100-fold higher drug load in the donor formulations, the plateaus of donor emulsion and suspension were at the same level (~44%, 0.15 mg = 100%). As for the low concentration, the highest transfer was displayed by the donor liposomes (~50%). The transfer rate decreased from donor emulsion to suspension to liposomes.

The donor formulations containing the high temoporfin concentration (1.5 mg/mL) were utilized for additional transfer experiments using different donor–acceptor LMRs. This was achieved by mixing the donor formulations with increasing amounts of acceptor emulsion. Although the dispersed lipophilic acceptor phase also leads to dilution, these experiments are not comparable to the highly water-diluted experiments investigating Nile red transfer.

Increasing the  $\text{LMR}_{\text{real}}$  to 1 + 112 (DoEmu/DoSusp) and to 1 + 125 (DoLip) led to an increased amount of transferred temoporfin (Figure 3C, Table 5, Supplemental Figure VI in the Supporting Information). Assuming an equal temoporfin distribution between donor and acceptor, a slight increase (from 96 to 99%) of the nominal temoporfin fraction in the acceptor emulsion was expected. For donor emulsion and suspension the plateau level was, however, only around 63%. The plateau for the donor liposomes was markedly higher (~75%). Again, the transfer from the liposomes was slower than from the nanoparticles. For the higher LMR all donor formulations showed a slightly faster transfer. A further increase of the  $\text{LMR}_{\text{real}}$  to 1 + 223 (DoEmu/DoSusp) or to 1 + 250 (DoLip) resulted in a further but smaller increase of the transferred amount of temoporfin (Figure 3D, Table 5, Supplemental Figure VI in the Supporting Information). In this experiment, at most 99.6% of the introduced dye would theoretically be expected within the acceptor. However, the slightly decelerated transfer from donor emulsion and suspension was terminated at a plateau level between 68 to 72%. Once more, the transfer from the donor liposomes ended at the highest plateau level (~88%) but was also the slowest of all three donor formulations.

**Investigation of Nile Red Transfer into a Layer of Liquid Oil (Well Plate Transfer Study).** The Nile red transfer from donor emulsion and suspension was investigated by measuring the Nile red fluorescence intensity in an acceptor cover layer of medium chain triglycerides pipetted on top of the nanoparticle dispersions. Compared to the very

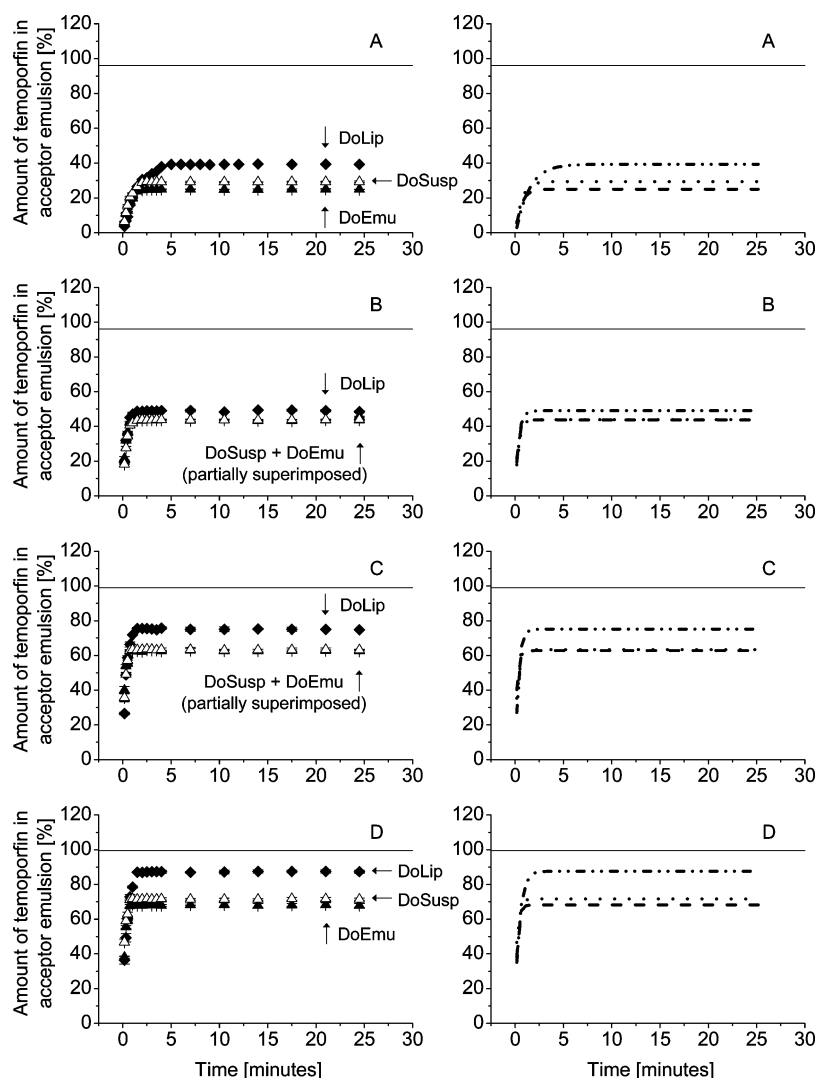


**Figure 3.** Transfer of temoporfin from donor nanoparticles and donor liposomes to acceptor emulsion at different  $LMR_{nom}$ . 100% dye in AcEmu correspond to 1.5  $\mu\text{g}$  (A) or 0.15 mg (B to D) temoporfin. Measurement results (left,  $n = 3$ ), fitted curves (right),  $\blacktriangle$  or dashed line = DoEmu,  $\triangle$  or dotted line = DoSusp,  $\blacklozenge$  or dashed-dotted line = DoLip, continuous line = equal distribution of temoporfin between donor and acceptor. (A) low temoporfin concentration,  $LMR_{nom}$  1 + 25 ( $LMR_{real}$  1 + 22 for DoEmu/DoSusp, 1 + 25 for DoLip). (B) high temoporfin concentration,  $LMR_{nom}$  1 + 25 ( $LMR_{real}$  1 + 22 for DoEmu/DoSusp, 1 + 25 for DoLip). (C) high temoporfin concentration,  $LMR_{nom}$  1 + 125 ( $LMR_{real}$  1 + 112 for DoEmu/DoSusp, 1 + 125 for DoLip). (D) high temoporfin concentration,  $LMR_{nom}$  1 + 250 ( $LMR_{real}$  1 + 223 for DoEmu/DoSusp, 1 + 250 for DoLip). Some results are superimposed (rising part of the curves, DoEmu and DoSusp in B and C). For further details see Table 5.

rapid transfer into a dispersed oil phase in the form of acceptor emulsion droplets, the transfer into the nondispersed bulk phase was complete but very slow (Figure 4, Table 3). The initially introduced Nile red ( $0.8 \mu\text{g} = 100\%$ ) had transferred after approximately 50 or 100 h for the donor suspension and emulsion, respectively.

**Ultracentrifugation of Donor–Acceptor Mixtures Containing DiI.** Additionally, the DiI transfer was investigated in ultracentrifugation studies for which a donor suspension was mixed with acceptor emulsions of different median particle sizes ( $LMR_{real}$  1 + 22). The mixtures could easily be separated by centrifugation with the solid donor suspension platelets forming a pellet and the liquid acceptor emulsion droplets floating on top as a cream layer. The

centrifugation of mixtures containing large acceptor droplets led to noncolored acceptor cream layers and dark pink donor particle pellets indicating a lack of transfer. The centrifugation of mixtures containing small acceptor droplets led to light pink acceptor cream layers and light pink donor particle pellets indicating dye transfer.

To evaluate these findings in more detail, the pellets were dissolved and DiI absorbance was measured to determine the fraction of dye remaining in the pellet. An adhesion effect of PVA introduced by the acceptor emulsions complicated the sample transfer from centrifugation tubes into glass vials. This caused a dye loss, which, estimated by the recovery test (91%), was about 9%. Thus the results have to be regarded as semiquantitative. The recovery test was only

**Table 5.** Comparison of the Finally Transferred Percentual Amount of Temoporfin ( $A_{\text{final}}$ ) and the Rate Constants ( $k$ ) for Temoporfin Transfer into Acceptor Emulsions Using Different Temoporfin Concentrations in the Donor Formulations and Different Donor–Acceptor Lipid Mass Ratios (LMR)

type of experiment	formulations used	donor emulsion	donor suspension	donor liposomes
different temoporfin concentrations in the donor formulations, $\text{LMR}_{\text{nom}}$ as usual (1 + 25) <sup>b</sup>			$A_{\text{final}}$ [%] <sup>a</sup>	
$c = 15 \mu\text{g/mL}$	DoEmu/DoSusp-3-Tem and DoLip-2-Tem to AcEmu-4	$25.0 \pm 0.6$	$29.4 \pm 0.5$	$39.4 \pm 1.0$
$c = 1.5 \text{ mg/mL}^c$	DoEmu/DoSusp-3-Tem and DoLip-3-Tem to AcEmu-4	$43.7 \pm 0.6$	$43.8 \pm 0.5$	$49.0 \pm 1.0$
			$k$ [ $\text{min}^{-1}$ ] <sup>a</sup>	
$c = 15 \mu\text{g/mL}$	DoEmu/DoSusp-3-Tem and DoLip-2-Tem to AcEmu-4	$1.7 \pm 0.3$	$1.6 \pm 0.2$	$0.7 \pm 0.1$
$c = 1.5 \text{ mg/mL}^c$	DoEmu/DoSusp-3-Tem and DoLip-3-Tem to AcEmu-4	$3.9 \pm 0.8$	$3.1 \pm 0.4$	$2.9 \pm 0.7$
different donor–acceptor $\text{LMR}_{\text{nom}}^c$			$A_{\text{final}}$ [%] <sup>a</sup>	
1 + 125 <sup>d</sup>	DoEmu/DoSusp-3-Tem and DoLip-3-Tem to AcEmu-4	$62.8 \pm 1.0$	$63.4 \pm 0.7$	$75.2 \pm 0.9$
1 + 250 <sup>e</sup>	DoEmu/DoSusp-3-Tem and DoLip-3-Tem to AcEmu-4	$68.2 \pm 1.1$	$71.7 \pm 1.0$	$87.6 \pm 1.2$
			$k$ [ $\text{min}^{-1}$ ] <sup>a</sup>	
1 + 125 <sup>d</sup>	DoEmu/DoSusp-3-Tem and DoLip-3-Tem to AcEmu-4	$4.6 \pm 1.7$	$4.5 \pm 0.8$	$3.2 \pm 0.4$
1 + 250 <sup>e</sup>	DoEmu/DoSusp-3-Tem and DoLip-3-Tem to AcEmu-4	$4.6 \pm 1.3$	$3.9 \pm 1.2$	$2.1 \pm 0.3$

<sup>a</sup> Fitted mean and standard deviation. <sup>b</sup>  $\text{LMR}_{\text{real}}$  1 + 22 (DoEmu/DoSusp) and 1 + 25 (DoLip). <sup>c</sup> Temoporfin concentration of 1.5 mg/mL in DoEmu/DoSusp and of 1.3 mg/mL in DoLip. <sup>d</sup>  $\text{LMR}_{\text{real}}$  1 + 112 (DoEmu/DoSusp) and 1 + 125 (DoLip). <sup>e</sup>  $\text{LMR}_{\text{real}}$  1 + 223 (DoEmu/DoSusp) and 1 + 250 (DoLip).

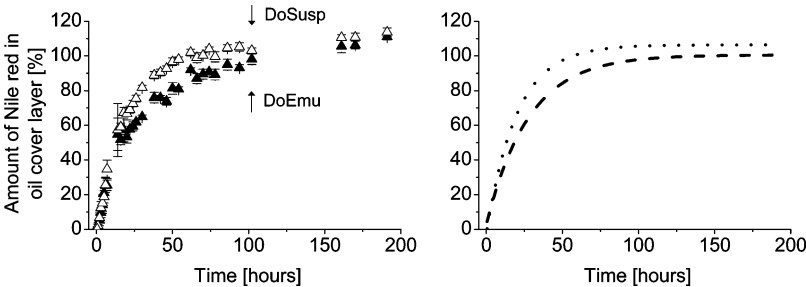


**Figure 4.** Transfer of Nile red from donor nanoparticles into a layer of medium chain triglycerides ( $\text{LMR}_{\text{nom}}$  1 + 100,  $\text{LMR}_{\text{real}}$  1 + 90). 100% dye in the acceptor phase correspond to 0.8  $\mu\text{g}$  Nile red. Measurement results (left,  $n = 9$ ), fitted curves (right),  $\blacktriangle$  or dashed line = DoEmu,  $\triangle$  or dotted line = DoSusp. In the rising part of the curves some results are superimposed. For further details see Table 3.

performed for comparative purposes (the results were not corrected for the dye loss). Nevertheless, they still provide a good overview on the differences related to shaking time and particle size of the acceptor emulsion (Figure 5). Mixing donor suspension with small acceptor droplets led to a low DiI content in the donor pellet already after shaking for 6 h which did not change during shaking for 32 days (= fast and pronounced transfer). An increase in acceptor droplet size resulted in an increase in the remaining DiI content in the donor pellet (= extent of transfer decreased). For these larger acceptor droplets, after 32 days, a lower DiI content was determined in the donor suspension pellet compared to 6 h (= continued transfer during extended shaking). The transfer into the acceptor droplets larger than 1  $\mu\text{m}$  was not very pronounced (6 h of shaking, <15%; 32 days of shaking, <35%).

Discussion

**Use of Flow Cytometry for Studies on Drug Release and Transfer.** While flow cytometry is predominantly being used for cell studies, its use has also been documented for

characterization of lipid particles like liposomes and emulsion droplets.<sup>16,18,32</sup> In the present study, it was employed to monitor the transfer of fluorescent model substances from lipidic colloidal donor carriers into larger acceptor o/w emulsion droplets which are intended to mimic acceptor sites present in the bloodstream.

The major advantage of this method, compared to techniques like e.g. ultrafiltration or centrifugation, is the absence of any separation procedures of donor and acceptor particles.<sup>1</sup> Combining several measurement protocols starting at different time points after mixing donor and acceptor, a reasonable time resolution can be achieved, which is often a problem with other techniques.<sup>1</sup> A good reproducibility was found in control experiments conducted with Nile red and lipid nanoparticles (see Supporting Information and Supplemental Figure III in the Supporting Information).

One limitation of the presented method is the minimal size requirement for the acceptor particles in the lower  $\mu\text{m}$  range.

(32) Vorauer-Uhl, K.; Wagner, A.; Borth, N.; Katinger, H. Determination of liposome size distribution by flow cytometry. *Cytometry* **2000**, *39*, 166–171.

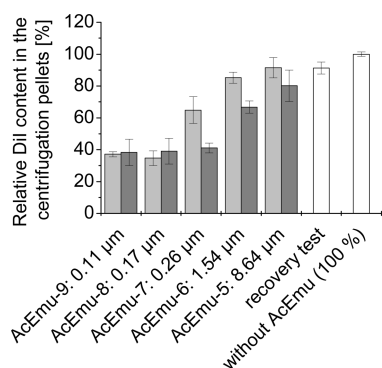


**Figure 5.** Dil content in the centrifugation pellets (DoSusp-5-Dil). The relative percentual amount is related to the absorbance of the sample “without AcEmu” being 100% ( $n = 3$ ). White = centrifugation directly after mixing, light gray = centrifugation after 6 h, dark gray = centrifugation after 32 days, AcEmu-9 to AcEmu-5 = mixtures containing DoSusp and AcEmus with increasing median droplet size, recovery test = mixture containing DoSusp and AcEmu-5, without AcEmu (100%) = reference value, centrifugation of DoSusp without acceptor emulsion.

Therefore, a transfer into nanosized blood components (e.g., serum proteins, platelets) cannot be measured. The stability of the used acceptor formulation might also become a critical factor, as the particles used so far are prone to coalesce, e.g. during long-term experiments or in high dilution. Another drawback is that the selection of drugs is limited to fluorescent compounds.

In summary, we were able to show that flow cytometry is a very useful method to evaluate general drug transfer principles provided that certain preconditions are fulfilled. Although the results obtained during these investigations are not yet elaborated enough to draw definite conclusions about the release or transfer mechanisms, they give important insights into the transfer behavior of lipophilic substances.

#### Transfer of Nile Red into Acceptor Emulsion Droplets.

We observed a rapid transfer of Nile red in the undiluted mixtures which is in agreement with the conclusions on Nile red transfer from poly(lactic-co-glycolic acid) (PLGA) nanoparticles to cells.<sup>33,34</sup> Dilution led to decreased transfer rates and, at the highest dilution, to lower plateau values. According to previous results, drug transfer between lipophilic particles may occur via collision of donor and acceptor particles or via diffusion through the aqueous phase. Collision transfer has been described, e.g., between colloidal carrier

particles and cells<sup>35,36</sup> and diffusion transfer was shown for fluorescent lipids.<sup>37,38</sup> Optionally, both mechanisms may proceed simultaneously.<sup>33,34,36</sup> In principle, the observation of a rapid transfer in the undiluted mixtures and a decreased transfer rate in the diluted mixtures is consistent with a collision transfer mechanism as a reduced particle density should lead to fewer collisions. The polymer chains sterically stabilizing the donor nanoparticles (polyoxyethylene chains of poloxamer 188) and the acceptor emulsion (PVA) should, however, counteract collisions by preventing a direct contact of the lipid particles. Consequently, the dye would have to move along the polymer chains in order to transfer. Nile red diffusion through the aqueous phase may thus be a more conceivable transfer mechanism especially since Nile red has a non-negligible water solubility.<sup>39</sup> Shorter diffusion paths in the undiluted mixtures should lead to a faster transfer than in the diluted mixtures with longer diffusion paths. However, a final determination of the type of transfer mechanism on this stage of the investigations is difficult. Factors like partitioning or drug solubility in the release medium and in the donor formulation are also of importance.<sup>40</sup> Thus, the decreased amount of transferred Nile red in the most diluted mixture might result from its additional partitioning into the aqueous phase where its fluorescence is quenched.<sup>39</sup>

The transfer behavior of Nile red, particularly considering the plateau level, was not only influenced by dilution but also by the donor formulation. In any case, more dye was transferred from donor liposomes than from donor lipid nanoparticles. Typically, Nile red is used to label triglyceride containing cytoplasmatic lipid droplets.<sup>41</sup> Its high affinity to such lipids present in both donor lipid nanoparticles and acceptor emulsion may explain the almost equal dye distribution between these particles. Its lower affinity to the liposomal phospholipid membrane led to a more pronounced

- (33) Pietzonka, P.; Rothen-Rutishauser, B.; Langguth, P.; Wunderli-Allenspach, H.; Walter, E.; Merkle, H. P. Transfer of Lipophilic Markers from PLGA and Polystyrene Nanoparticles to Caco-2 Monolayers Mimics Particle Uptake. *Pharm. Res.* **2002**, *19*, 595–601.
- (34) Xu, P.; Gullotti, E.; Tong, L.; Highley, C. B.; Errabelli, D. R.; Hasan, T.; Cheng, J. X.; Kohane, D. S.; Yeo, Y. Intracellular drug delivery by poly(lactic-co-glycolic acid) nanoparticles, revisited. *Mol. Pharmaceutics* **2009**, *6*, 190–201.

- (35) Haynes, L. C.; Cho, M. J. Mechanism of Nile red transfer from o/w (oil-in-water) emulsions as carriers for passive drug targeting to peritoneal macrophages in vitro. *Int. J. Pharm.* **1988**, *45*, 169–177.
- (36) Yang, E.; Huestis, W. H. Mechanism of intermembrane phosphatidylcholine transfer: effects of pH and membrane configuration. *Biochemistry* **1993**, *32*, 12218–12228.
- (37) Roseman, M. A.; Thompson, T. E. Mechanism of the spontaneous transfer of phospholipids between bilayers. *Biochemistry* **1980**, *19*, 439–444.
- (38) Doody, M. C.; Pownall, H. J.; Kao, Y. J.; Smith, L. C. Mechanism and kinetics of transfer of a fluorescent fatty acid between single-walled phosphatidylcholine vesicles. *Biochemistry* **1980**, *19*, 108–116.
- (39) Greenspan, P.; Fowler, S. D. Spectrofluorometric studies of the lipid probe, Nile red. *J. Lipid Res.* **1985**, *26*, 781–789.
- (40) Yang, S.; Washington, C. Drug release from microparticulate systems. In *Drugs and the Pharmaceutical Sciences 158 (Microencapsulation—Methods and Industrial Applications)*, 2nd ed.; Benita, S., Ed.; CRC Press: Boca Raton, 2006; pp 183–211.
- (41) Greenspan, P.; Mayer, E. P.; Fowler, S. D. Nile red: a selective fluorescent stain for intracellular lipid droplets. *J. Cell Biol.* **1985**, *100*, 965–973.



transfer from donor liposomes. This was also observable for the drug temoporfin.

In some cases small differences between the transferred amounts of Nile red (and of the other dyes under investigation) from the two lipid nanoparticle formulations were observed. In diluted mixtures, Nile red transferred to a larger extent from the donor suspension than from the donor emulsion. This might result from the larger surface area for collision contacts or for diffusion presented by the plateletlike crystalline suspension particles compared to the spherically shaped emulsion particles.<sup>6,42</sup> Dye expulsion during lipid crystallization may also play a role.<sup>6,24,26,28,42</sup> Thus, collision or diffusion transfer would both benefit from a dye enrichment in the surface region of the donor suspension platelets.

**Flow Cytometric Investigations with Dyes of Higher Lipophilicity.** Lipophilicity of the dyes was obviously one of the determining factors for the transfer behavior. Lipophilicity was estimated according to the log *P* calculated for Nile red and temoporfin (ACD/ChemSketch Freeware 11.01, Advanced Chemistry Development Inc., Toronto, Canada) or found in the literature for DiI.<sup>43</sup> The log *P* values increase from Nile red ( $3.65 \pm 1.37$ ) to temoporfin ( $9.17 \pm 1.53$ ) to DiI (20.0). The quite high lipophilicity of DiI might have contributed to its slow transfer completing at a low acceptor plateau level. Poor water solubility and an amphiphilic character (due to two C<sub>18</sub> alkyl chains) counteract partitioning of DiI into the aqueous phase and probably lead also to strong interactions with the donor trimyristin matrix.<sup>44</sup> A DiI enrichment in the particle interface is most likely, but only few molecules may transfer by diffusion into the acceptor. This high affinity of DiI to lipophilic particles is used to label lipoproteins like e.g. LDL or cellular membranes without the need of a covalent link.<sup>21,22,44</sup> For temoporfin, according to its lipophilicity, a transfer behavior (rate, amount of transferred dye) between that of Nile red and DiI was expected. Interestingly, compared to Nile red, only a slightly lower transfer rate but a much lower plateau level was determined for temoporfin (15 µg/mL). The plateau levels increased from donor emulsion to suspension to liposomes. According to literature, liposomes can directly deliver a drug to lipoproteins thus serving as drug donor.<sup>45,46</sup> The rapid transfer of a larger drug fraction might be explained by the location of the drug near the liposome surface, as this drug

like many others is perturbing the lipid bilayer.<sup>47</sup> Furthermore, as observed for Nile red, temoporfin appears to have a higher affinity to apolar lipids explaining the less pronounced transfer from the donor lipid nanoparticles.<sup>46</sup>

The transfer of DiI and temoporfin equilibrates at lower plateau concentrations compared to Nile red. Since both substances have a more or less amphiphilic character they might preferably accumulate in the particle interface.<sup>44,48</sup> Thus, the low plateau level might originate from a saturation of the limited surface area of the large acceptor droplets as was observed for DiI during ultracentrifugation (see below).

For DiI, slightly different incubation temperatures led to different transfer curve characteristics. Incubation at room temperature resulted in single exponential transfer curves whereas incubation at 37 °C led to a relatively high transfer during the first day and a sigmoidal-like transfer curve from the donor suspension. Hitherto, we do not have a conclusive explanation for this behavior. A higher dye mobility in the lipid matrix at elevated temperatures might have an impact or, as observable in DSC measurements, a small fraction of the donor suspension particles may already be melting at 37 °C. The first molecules to be transferred probably originate from the particle surface (rapid transfer during the first days), and the remaining dye may undergo a rearrangement in the particles leading to a slow transfer as also observed at 23 °C. A definition of the thermal conditions during release or transfer studies is thus of high importance, even though the difference was only a few degrees centigrade in our case. In order to approach *in vivo* conditions more closely, future transfer studies should be performed at 37 °C.

The results obtained with higher temoporfin loads demonstrate that the drug content in the donor can have an impact on the release behavior. A 100-fold increase in drug load significantly increased the transfer rate and also the amount of transferred temoporfin. This might be attributed to drug interactions with the structure of the particle matrix as indicated by DSC results (see Supporting Information; high drug load changes lipid polymorphism). Furthermore, a modified dye distribution toward the particle interface (after exclusion from the matrix) might play a role as well as the presence of a small fraction of temoporfin crystals in the donor nanoparticle formulations (see Supporting Information).

The transfer behavior depended also on the LMR between acceptor and donor. With increasing amounts of acceptor

(42) Jores, K.; Haberland, A.; Wartewig, S.; Mäder, K.; Mehnert, W. Solid lipid nanoparticles (SLN) and oil-loaded SLN studied by spectrofluorometry and Raman spectroscopy. *Pharm. Res.* **2005**, *22*, 1887–1897.

(43) Rashid, F.; Horobin, R. W. Interaction of molecular probes with living cells and tissues. Part 2. A structure-activity analysis of mitochondrial staining by cationic probes, and a discussion of the synergistic nature of image-based and biochemical approaches. *Histochemistry* **1990**, *94*, 303–308.

(44) Haugland, R. P. Dialkylcarbocyanine and dialkylaminostyryl probes. In *The Handbook: A Guide to Fluorescent Probes and Labeling Technologies*, 10th ed.; Spence, M. T. Z., Ed.; Invitrogen Corp.: Eugene, 2005; pp 624–627.

(45) Derycke, A. S. L.; de Witte, P. A. M. Liposomes for photodynamic therapy. *Adv. Drug Delivery Rev.* **2004**, *56*, 17–30.

(46) Konan, Y. N.; Gurny, R.; Allémann, E. State of the art in the delivery of photosensitizers for photodynamic therapy. *J. Photochem. Photobiol. B* **2002**, *66*, 89–106.

(47) Fahr, A.; van Hoogevest, P.; May, S.; Bergstrand, N.; Leigh, M. L. S. Transfer of lipophilic drugs between liposomal membranes and biological interfaces: Consequences for drug delivery. *Eur. J. Pharm. Sci.* **2005**, *26*, 251–265.

(48) Wiehe, A.; Shaker, Y. M.; Brandt, J. C.; Mebs, S.; Senge, M. O. Lead structures for applications in photodynamic therapy. Part 1: Synthesis and variation of m-THPC (Temoporfin) related amphiphilic A2BC-type porphyrins. *Tetrahedron* **2005**, *61*, 5535–5564.

compared to donor lipid, the amount of transferred temoporfin increased. This was anticipated assuming a mass equilibrium of the dye between donor and acceptor. Nominally, the three investigated LMRs would lead to equilibria close to 100% (= approximately 100% of the dye transferred to the acceptor). This was, however, not even reached with the highest LMR in our experiments. Besides a simple mass equilibrium law, structural properties of the particles during desorption and adsorption will play a role (e.g., saturation of binding places at the acceptor particle surface).

**Transfer Results with Alternative Methods.** Due to a low time resolution, separation of donor and acceptor particles by ultracentrifugation could only be applied to the slowly transferring DiI and not for the rapid transfer of Nile red or temoporfin. On the other hand, investigations with smaller sized acceptor droplets ( $<0.5\ \mu\text{m}$ ) are not feasible using flow cytometry. The ultracentrifugation study revealed interdependencies between acceptor surface area and amount of transferred dye. DiI transferred rapidly and to a large extent from the donor suspension into small sized acceptor droplets possessing a large specific surface area. In good agreement with the flow cytometric results, the transfer into large acceptor droplets with a small specific surface area was very slow and weak. For large surface area ratios, the DiI transfer is expected to converge to a limit value. With regard to the application of DiI as a fluorescent label (e.g., to trace colloidal particles on their way into cells) it is an important result that the transfer from DiI labeled particles into large acceptor structures (e.g., cells) takes place only slowly.<sup>49</sup>

In addition to the flow cytometric studies of Nile red with a dispersed lipophilic acceptor, we also investigated the transfer into a nondispersed bulk phase. Such lipophilic bulk acceptor media have been used previously to study drug release from colloidal carrier particles which was found to be very slow.<sup>25,50</sup> Our study revealed a complete but much slower Nile red transfer compared to flow cytometry which was probably caused by the larger  $\text{LMR}_{\text{nom}}$  ( $1 + 100$  instead of  $1 + 25$  for flow cytometry) and the smaller interfacial area ( $2\ \text{cm}^2$  vs  $500\ \text{cm}^2$  for flow cytometry). This small interfacial area, the longer diffusion pathways and a limited agitation generate a very slow, retarded transfer into the bulk lipid which would not be observed under more physiological conditions which we tried to mimic in the flow cytometric studies.

## Conclusion

A flow cytometry method was developed to investigate the transfer of fluorescent dyes from colloidal donor particles (lipid nanoparticles, liposomes) into large o/w acceptor

emulsion droplets. Compared to commonly applied release methods, the use of dispersed lipophilic acceptor particles in the same compartment is a better approach to the conditions in blood, e.g. after iv injection. This method has a very good time resolution and does not require the critical step separating donor and acceptor particles. It is suitable to investigate fast as well as very slow transfer processes. We could demonstrate advantages compared to earlier attempts of studying drug transfer into lipophilic bulk phases. The method will not be applicable for most drugs, since it relies on fluorescence detection. It does, however, allow elucidation of the general phenomenon of drug transfer with the help of fluorescent model substances. A dependence between transfer behavior and drug lipophilicity in the order Nile red (low lipophilicity, fast and pronounced transfer), temoporfin (medium lipophilicity, fast and moderate transfer), and DiI (high lipophilicity, slow transfer to a minor extent) was observed. The transfer from liposomes was more pronounced than from lipid nanoparticles, and the differences between donor suspension and emulsion were rather small. The transfer strongly depended on experimental conditions like dilution in water, drug load in the donor formulations, and amount of acceptor lipid. A relation between transfer characteristics and the size of the acceptor surface area was also observed. This effect was particularly evident from the ultracentrifugation experiments and calls for further investigations. Moreover, in order to clearly determine all influential factors on the transfer behavior, more dyes with different physicochemical properties need to be investigated. Variations in the experimental setup are recommendable as well as the help of other techniques. Nevertheless, we can conclude that flow cytometry is a suitable tool to investigate the basic transfer principles of fluorescent model substances or fluorescent drugs into cell-sized particles coming close to transfer processes occurring in blood.

## Abbreviations Used

O/w, oil-in-water; AcEmu, acceptor emulsion; DoEmu, donor emulsion; DoSusp, donor suspension; DoLip, donor liposomes; NR, Nile red; DiI, DiI<sub>C18</sub>(3); Temo, temoporfin; LMR, lipid mass ratio;  $\text{LMR}_{\text{nom}}$ , nominally intended lipid mass ratio;  $\text{LMR}_{\text{real}}$ , actually applied lipid mass ratio;  $A_{\text{acc}}$ , percental amount of dye transferred to acceptor emulsion;  $A_{\text{final}}$ , final percental amount of dye transferred to acceptor emulsion;  $A_0$ , percental amount of dye transferred to acceptor emulsion at time zero;  $A$ , pre-exponential coefficient;  $k$ , transfer rate constant;  $t$ , time; PI, polydispersity index.

**Acknowledgment.** We thank J. M. Gasch for performing preliminary tests.

**Supporting Information Available:** Supplemental methods, results, table and figures. This material is available free of charge via the Internet at <http://pubs.acs.org>.

MP900130S

(49) Verma, D. D.; Verma, S.; Blume, G.; Fahr, A. Particle size of liposomes influences dermal delivery of substances into skin. *Int. J. Pharm.* **2003**, 258, 141–151.

(50) Wissing, S. A.; Müller, R. H. Solid lipid nanoparticles as carrier for sunscreens: in vitro release and in vivo skin penetration. *J. Controlled Release* **2002**, 81, 225–233.